Atmospheric Environment 92 (2014) 429–441

Contents lists available at ScienceDirect

Atmospheric Environment

journal homepage: www.elsevier.com/locate/atmosenv

Relationship between column-density and surface mixing ratio: Statistical analysis of O_3 and NO_2 data from the July 2011 Maryland DISCOVER-AQ mission

Clare M. Flynn [a,*], Kenneth E. Pickering [a,b], James H. Crawford [c], Lok Lamsal [d], Nickolay Krotkov [b], Jay Herman [e], Andrew Weinheimer [f], Gao Chen [c], Xiong Liu [g], James Szykman [h], Si-Chee Tsay [b], Christopher Loughner [i], Jennifer Hains [j], Pius Lee [k], Russell R. Dickerson [a], Jeffrey W. Stehr [a], Lacey Brent [a]

[a] Department of Atmospheric and Oceanic Science, University of Maryland, College Park, MD 20742, United States
[b] NASA Goddard Space Flight Center, United States
[c] NASA Langley Research Center, United States
[d] GESTAR, NASA Goddard Space Flight Center, United States
[e] UMBC, NASA Goddard Space Flight Center, United States
[f] NCAR Atmospheric Chemistry Division, United States
[g] Harvard-Smithsonian Center for Astrophysics, United States
[h] EPA, Office of Research and Development, United States
[i] ESSIC-NASA Goddard Space Flight Center, United States
[j] Maryland Department of the Environment, United States
[k] NOAA Air Resources Laboratory, United States

HIGHLIGHTS

- O_3 presented much larger correlation between column and surface data than NO_2 data.
- A simple linear regression model fit the O_3 column and surface data well.
- PBL height adds useful information to the regressions for both gases.
- CMAQ correlations were similar to data for O_3, but often larger for NO_2.
- CMAQ displays greater influence of mixing on correlations than the data.

ARTICLE INFO

Article history:
Received 26 November 2013
Received in revised form
21 April 2014
Accepted 23 April 2014
Available online 26 April 2014

Keywords:
Ozone
Nitrogen oxides
DISCOVER-AQ
Column–surface relationship
Aircraft measurement campaign
Measurement-model comparison

ABSTRACT

To investigate the ability of column (or partial column) information to represent surface air quality, results of linear regression analyses between surface mixing ratio data and column abundances for O_3 and NO_2 are presented for the July 2011 Maryland deployment of the DISCOVER-AQ mission. Data collected by the P-3B aircraft, ground-based Pandora spectrometers, Aura/OMI satellite instrument, and simulations for July 2011 from the CMAQ air quality model during this deployment provide a large and varied data set, allowing this problem to be approached from multiple perspectives. O_3 columns typically exhibited a statistically significant and high degree of correlation with surface data ($R^2 > 0.64$) in the P-3B data set, a moderate degree of correlation ($0.16 < R^2 < 0.64$) in the CMAQ data set, and a low degree of correlation ($R^2 < 0.16$) in the Pandora and OMI data sets. NO_2 columns typically exhibited a low to moderate degree of correlation with surface data in each data set. The results of linear regression analyses for O_3 exhibited smaller errors relative to the observations than NO_2 regressions. These results suggest that O_3 partial column observations from future satellite instruments with sufficient sensitivity to the lower troposphere can be meaningful for surface air quality analysis.

* Corresponding author.
E-mail address: cflynn@atmos.umd.edu (C.M. Flynn).

http://dx.doi.org/10.1016/j.atmosenv.2014.04.041
1352-2310/

1. Introduction

Satellite observations have made important contributions to the understanding of atmospheric chemistry and pollution over the past three decades, including quantifying the atmospheric abundances and distributions of many trace gas species, assessing temporal trends in these species, and top-down estimates of trace gas emissions (Fishman et al., 2008). Global coverage, coupled with increasingly high spatial resolution, and fixed temporal resolution of such observations provide key advantages over other data sets. Retrievals of tropospheric column abundances have also improved (Beirle et al., 2003; Boersma et al., 2008; Bucsela et al., 2013; Chatfield and Esswein, 2012; Fishman et al., 2008; Martin, 2008; Lamsal et al., 2011). Trace gas observations from satellites thus have great potential for diagnosis of near-surface conditions. This can be especially useful for monitoring the Environmental Protection Agency (EPA) criteria pollutants ozone (O_3) and nitrogen dioxide (NO_2) (http://www.epa.gov/air/criteria.html), pollutants known to have significant adverse impacts on human health, crop yields, and the atmospheric radiation budget. The greatest benefit may come in regions that lack sufficient surface air quality monitors.

However, several factors currently complicate the applicability of satellite-observed column abundances for surface air quality assessment. These include biases in satellite retrievals and reduced sensitivity of satellite instruments to the lower troposphere (Martin, 2008; Lee et al., 2011). Just as importantly, uncertainties remain in the relationship between column abundances observed by satellites and surface mixing ratios, which are directly relevant to air quality management. Recent work demonstrates progress in understanding this relationship. Chatfield and Esswein (2012) analyzed ozonesonde data over the U. S. and found substantial correlation between partial-column O_3 (0–3 km) and near-surface O_3 (in the lowest 500 m). Lamsal et al. (2008) developed a method to infer ground-level NO_2 mixing ratios from the Ozone Monitoring Instrument (OMI) tropospheric column abundances with the use of local scaling factors derived from the GEOS-Chem model. Significant correlation between OMI-derived and *in situ* surface NO_2 was observed (Lamsal et al., 2008, 2010). Other works have demonstrated significant correlation between satellite-observed NO_2 columns and surface NO_2 data scaled to obtain column amounts with the use of assumed NO_2 profiles (Ordóñez et al., 2006; Boersma et al., 2009). Knepp et al. (2013) used model-derived planetary boundary layer (PBL) heights to convert Pandora NO_2 tropospheric columns into average surface mixing ratios, also demonstrating high correlation between converted columns and surface data. Understanding the uncertainties in the relationship between column density and surface mixing ratio becomes more urgent with the up-coming NASA Tropospheric Emissions: Monitoring of Pollution satellite mission (TEMPO, Chance et al., 2012) which is likely to be one component of the Geostationary Coastal and Air Pollution Event (GEO-CAPE, Fishman et al., 2012) mission. TEMPO/GEO-CAPE will be centered over ~100° W, allowing observations over North America from geostationary orbit with product horizontal resolution of 8 km × 4.5 km at the center of domain, much higher than current Low-Earth-Orbit (LEO) measurements. GEO-CAPE may combine multiple spectral regions to improve the vertical resolution of ozone profile retrievals, especially in the lowermost troposphere (Natraj et al., 2011). However, because a number of retrieval assumptions will still be necessary, the challenge of relating the satellite-observed quantities to surface mixing ratios will remain.

The ultimate goal of the DISCOVER-AQ (Deriving Information on Surface conditions from Column and Vertically Resolved Observations Relevant to Air Quality) project is to provide information relevant to improving our ability to relate satellite-observed column densities to surface conditions for aerosols, O_3, NO_2, and CH_2O. Additional goals include characterization of differences in diurnal variability for surface and column observations and the horizontal scales of variability affecting satellites and model calculations. DISCOVER-AQ combines P-3B aircraft *in situ* profiling of trace gas species, aerosol properties, and key meteorological variables, UC-12 aircraft remote sensing of aerosols and trace gas columns below the aircraft, observations of surface conditions from the existing network of surface air quality monitors, remote sensing of trace gas columns and aerosols from a network of ground-based Pandora UV/vis spectrometers and a network of AERONET sun photometers collocated with the air quality monitors, and model simulations for the deployment period. The first deployment of this project was conducted in the Baltimore–Washington metropolitan region of Maryland during July 2011. The P-3B accomplished over 250 profiles on 14 flight days over six surface air quality monitoring sites and the Chesapeake Bay during the Maryland deployment. These flight days covered a range of conditions, including especially clean days on July 14th and 16th and pollution episodes during July 1–5 and July 18–23, as well as flights on weekdays and weekends.

In support of DISCOVER-AQ, results are presented of linear regression analyses between O_3 and NO_2 surface mixing ratio and column measurements, including column abundances integrated over *in situ* profile data from the P-3B aircraft, measured by the Pandora UV/vis spectrometer, and observed by the Aura/OMI instrument. Through these analyses, the strength of the column–surface relationship and the ability to predict simultaneous surface mixing ratio from column abundance during the July 2011 deployment will be assessed. The column–surface relationship in the CMAQ model is also evaluated and compared with the results obtained from the observations.

2. Data

A complete description of DISCOVER-AQ measurements is publicly available at http://www-air.larc.nasa.gov/cgi-bin/ArcView/discover-aq.dc-2011#2. The July 2011 campaign was conducted in the Baltimore–Washington metropolitan region and involved 6 surface air quality monitoring sites. These included Aldino, Beltsville, Edgewood, Essex, Fair Hill, and Padonia, MD, with locations mapped in Fig. 1. *In situ* trace gas volume mixing ratio data were collected by the P-3B aircraft over 14 flight days over these sites, with typically 3 spirals conducted over each surface site during each flight day. The National Center for Atmospheric Research (NCAR) $NO_{xy}O_3$ instrument, a 4-channel chemiluminescence instrument for the measurement of NO, NO_2, NO_y, and O_3 provided the P-3B O_3 and NO_2 *in situ* observations used here. Additional *in situ* flight observations were provided by the University of Maryland (UMD) Cessna 402B light aircraft (Taubman et al., 2004; He et al., 2014). Ozone was monitored with a TEI 49c UV photometry instrument (Thermo Environmental, Franklin, MA) and NO_2 by absorption in a cavity ringdown spectrometer (Los Gatos Research, Mountain View, CA). A ground-based Pandora UV/vis spectrometer (Herman et al., 2009) was located at each site, observing O_3 and NO_2 column amounts during daylight hours for all days in July. The Maryland Department of the Environment (MDE) provided the O_3 surface mixing ratio data at all sites, provided NO_2 measurements from a molybdenum-converter chemiluminescence monitor at Essex, and provided NO_y data from chemiluminescence monitors at Aldino and Beltsville. The EPA provided NO_2 measurements from chemiluminescence instruments with photolytic converters at Edgewood and Padonia, while the NASA mobile Chemical, Optical,

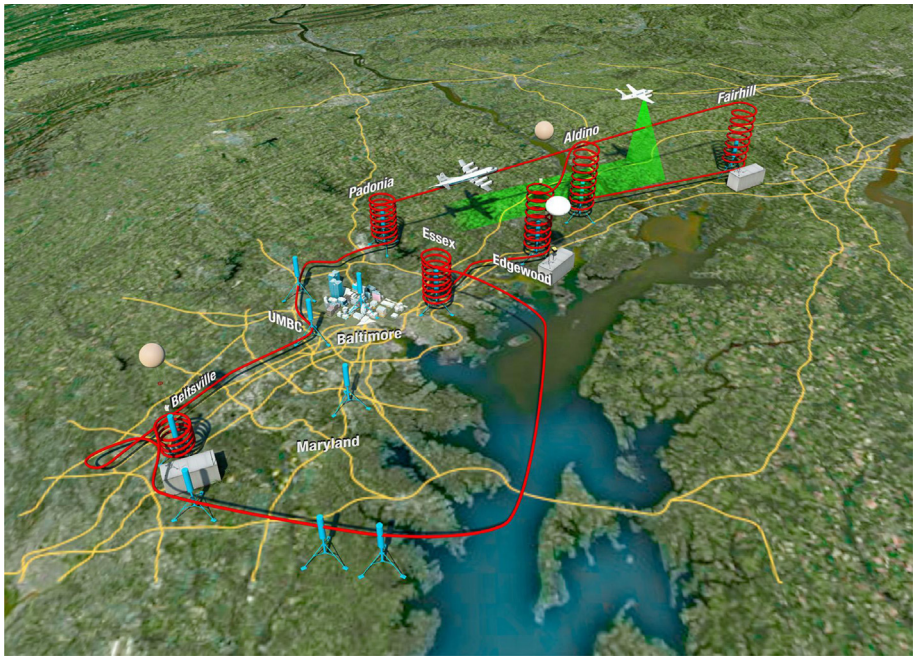

Fig. 1. Example P-3B flight track for the July 26th flight, displaying the locations of the 6 surface air quality monitoring sites.

and Microphysical Measurements of In-situ Troposphere (COMMIT; http://smartlabs.gsfc.nasa.gov) trailer provided photolytic converter measurements for Fair Hill.

3. WRF/CMAQ model runs

The Community Multiscale Air Quality (CMAQ) model Version 5.0 was used to simulate air quality for July 2011, as described by Loughner et al. (submitted for publication). CMAQ was fed output from the Weather Research and Forecasting meteorological model offline (WRF; Advanced Research WRF core; Skamarock et al., 2008). The WRF/CMAQ model system was run at 36 km, 12 km, 4 km, and 1.33 km horizontal resolution with 34 vertical layers from the surface to 100 mb, with 16 layers within the lowest 2 km to capture boundary layer processes. The WRF model used the Asymmetric Convective Model 2 (ACM2; Pleim, 2007) scheme for vertical diffusion and convective mixing, the Pleim-Xiu surface layer scheme (Pleim, 2006), and the Pleim-Xiu land surface model (Xiu and Pleim, 2001). The North American Regional Reanalysis (NARR) was used for the initial and lateral boundary conditions within WRF. Chemical initial and boundary conditions were provided by a simulation of the Model for Ozone and Related Chemical Tracers, version 4 (MOZART-4; Emmons et al., 2010). The CMAQ model used the Carbon Bond-05 (CB05; Yarwood et al., 2005) gas-phase chemical mechanism, the fifth generation aerosol model (aero5), the ACM2 for vertical diffusion and convective mixing, and used projected 2012 anthropogenic emissions based on the 2005 National Emissions Inventory (NEI) because 2011 emissions were not yet available. Lightning NO_x emissions were also included (Loughner et al., submitted for publication).

The Air Resources Laboratory of the National Oceanic and Atmospheric Administration (NOAA) provided forecasts of O_3 and NO_2 from an experimental version of CMAQ Version 4.6 during the deployment. The CB05 chemical mechanism was also used in the NOAA simulation. However, the NOAA model runs were driven offline by WRF (Nonhydrostatic Mesoscale Model core) meteorology, and used the fourth generation aerosol module (aero4), the Mellor–Yamada–Janjic (MYJ; Janjic, 1994) scheme for boundary layer and convective mixing, the Noah land surface model, and the 2005 NEI for anthropogenic emissions; lightning NO_x emissions were not included.

4. Analysis methods

4.1. Column abundance computation

In this work, two P-3B columns were computed for O_3 and NO_2, which differed by the method used to extend the aircraft profile data to the surface. Column_air was computed through integration of the profile after the mixing ratio measurement at the lowest aircraft altitude (at approximately 0.3 km AGL) was held constant from the lowest measurement altitude to the surface. Column_ground was computed in the same manner, but instead held the surface mixing ratio measurement constant up to the level of the lowest aircraft altitude, when a surface value was available. The top of the P-3B partial columns was typically at approximately 3 km.

The Aldino P-3B profile shapes were compared to *in situ* profile shapes measured by the UMD Cessna aircraft for O_3 and NO_2 during the campaign. The Cessna always reached lower altitudes than the P-3B, so this comparison was used to identify which P-3B column better approximated the true column at Aldino. The Cessna profiles for O_3 (Fig. 2) typically remained well mixed to the lowest Cessna altitude ($\sim$3 m AGL). Differences in O_3 measured by the Cessna and P-3B may be due to the different interferences experienced by the respective instruments after a spike in relative humidity (Arkinson et al., in preparation). The Cessna NO_2 profiles most often displayed a “boot shaped” appearance, with a sharp increase in NO_2 mixing ratio near the lowest P-3B altitude, then becoming better mixed in the lowest portion of the profile (Fig. 2). This suggests that generally column_air was closer to the true O_3 and NO_2 columns; however, due to the “boot” in the NO_2 profile, column_air likely underestimates the true NO_2 partial column. Additionally, these Cessna profiles were used to construct estimated profiles for the portion of the atmosphere below the lowest altitude of the Aldino P-3B spirals, and additional Aldino column amounts (column_UMD) were computed from these estimated profiles.

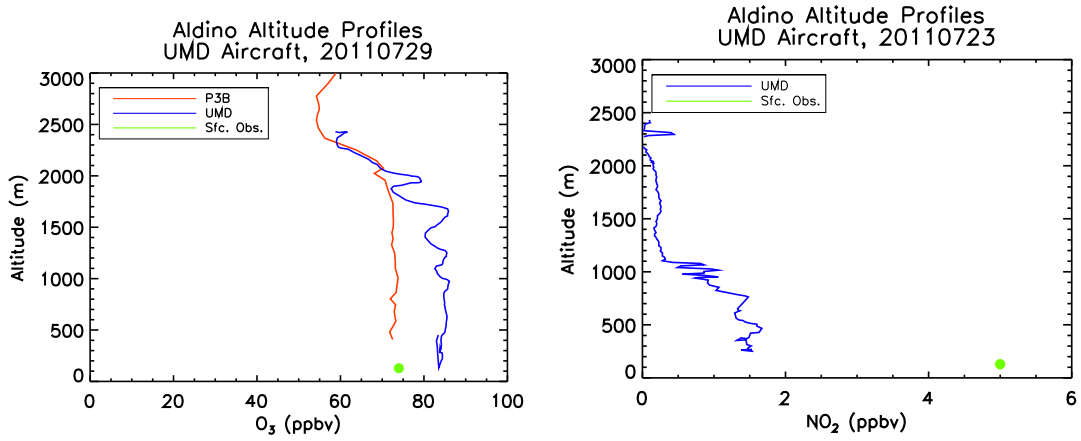

Fig. 2. Example UMD Cessna altitude profiles for Aldino. O_3 profile plotted in the left profile as solid blue line; NO_2 profile plotted in the right profile. NO_2 profile displays the "boot shaped" appearance. Corresponding P-3B profiles also plotted for comparison (orange). Green circles represent surface O_3 and NO_y mixing ratio data, measured at the nearby Aldino ground monitoring site, averaged over the time of UMD profile and plotted at the elevation AMSL of the monitoring site.

The 12 km horizontal resolution CMAQ output was used for the model analyses. Model column amounts for O_3 and NO_2 were computed through integration of the model profile from the model surface through the depth of the P-3B profiles for each site. OMI tropospheric columns were retrieved with the Version 2.1 Goddard tropospheric NO_2 retrieval algorithm (Bucsela et al., 2013) and the ozone profile algorithm by Liu et al. (2010) with modifications as described in Kim et al. (2013), and were screened for cloud fraction (effective cloud fraction less than 30%), the instrument row anomaly, and distance of the pixel center from the surface site (pixel center less than 100 km distance). Pandora tropospheric columns were estimated by subtracting the stratospheric component derived by the OMI algorithms from the Pandora total observed columns.

4.2. Molybdenum-converter instrument bias correction for NO_2

MDE used a molybdenum-converter chemiluminescence instrument to measure NO_2 at the Essex site. High biases in the Essex NO_2 data due to interferences from PAN and other NO_y species (Grosjean and Harrison, 1985; Demerjian, 2000; Dunlea et al., 2007; Steinbacher et al., 2007; Lamsal et al., 2008; Boersma et al., 2009) were corrected based upon comparison of the Edgewood EPA photolytic NO_2 measurements and the nearby Aberdeen Proving Grounds Mo-converter NO_2 measurements. First, the hourly mean bias of the Aberdeen measurements was computed as a percentage of the Edgewood EPA measurements, for each hour of the day over July 2011. These percentages were then used to determine correction factors with which to adjust the Mo-converter NO_2 measurement, so that these measurements better approximate photolytic NO_2 measurements. The Edgewood and Essex sites are approximately 20 miles apart, allowing the correction factors to be applied to the Essex Mo-converter NO_2 measurements.

The data for Aldino and Beltsville were measurements of NO_y and not NO_x, because the inlet did not remove HNO_3. It was not possible to develop a correction for these instruments at these sites, because no photolytic instruments were situated nearby.

4.3. Linear least squares regression analyses between column and surface data

4.3.1. Simple linear least squares regression analysis for the P-3B, Pandora, and OMI

A simple linear least squares regression analysis was performed between the P-3B column_air, P-3B column_ground, Pandora, and OMI O_3 and NO_2 columns and surface mixing ratio data for each surface-monitoring site. An additional analysis between the Aldino column_UMD and the surface data was also conducted for comparison to column_air and column_ground at this site. Surface data were averaged over the time of the aircraft spiral for use with the P-3B analyses. Hourly averages of the surface data for the hours between 7 AM and 7 PM EDT were computed for use with the Pandora columns, while 15 min averages centered on 2:45 PM EDT were computed for use with the OMI columns. Column abundance was used to predict the simultaneous surface mixing ratio, yielding a regression model of the form surface mixing ratio = β*(column) + intercept, where β is the regression coefficient. The NO_2 column and surface data followed an approximately lognormal distribution, and were therefore log-transformed before performing statistical analyses. The Pandora O_3 column data were also approximately lognormal, and were also log-transformed. The degree of association between the column and surface data and the errors of the regression model relative to the observed data were assessed.

4.3.2. Multivariate linear least squares regression analysis for the P-3B and Pandora

A multivariate linear least squares regression analysis was performed for P-3B column_air, column_ground, and Pandora O_3 and NO_2. Column abundance and inverse PBL height (1/PBLH) were used as predictor variables. The observational PBL height estimates were derived from the P-3B potential temperature spiral data. The PBL top was located where the potential temperature lapse rate exceeded approximately 3 K/km, with a relatively constant potential temperature lapse rate from the surface to the PBL top. This yielded an equation of the form surface mixing ratio = β_1*(column) + β_2*(PBL^{-1}) + intercept, where β_1 is the regression coefficient associated with the column, and β_2 is the regression coefficient associated with the inverse PBL height. To prevent limitation of the available Pandora columns, the Pandora analyses used PBL height estimates derived from the WRF/CMAQ model system. In the ACM2 PBL scheme, the PBL top is diagnosed as the height where the bulk Richardson number computed for the entrainment layer exceeds a critical value, typically set at 0.25.

4.4. Normalization by PBL height for the P-3B and Pandora

The degree of correlation between NO_2 column and surface mixing ratio was re-evaluated after normalization of the P-3B or

Pandora columns by the PBL height. Column abundances (molecules/cm^2) were divided by the concurrent PBL height (cm), yielding an estimate of mean number concentration in the PBL. The PBL height estimates derived from the P-3B potential temperature profile were used with the P-3B analyses, while the Pandora analyses again used PBL height estimates derived from the WRF/CMAQ model system. This approach is similar to that of Knepp et al. (2013), and allowed a comparison between the results presented here and those obtained by Knepp et al. (2013).

4.5. Comparison of CMAQ model column versus surface relationships to those from observations

A similar simple linear least squares regression analysis was applied to the Loughner et al. (submitted for publication) and NOAA CMAQ O_3 and NO_2 output to assess the correlation between column and surface within these model simulations. CMAQ model output was given in hourly increments. The NO_2 output was log-transformed before analysis. Additionally, correlation analyses for O_3 and NO_2 were also performed for several different conditions to further elucidate differences between the observations and the model. First, P-3B, Pandora, and CMAQ O_3 and NO_2 column and surface data were separated by the time of day at which they occurred, yielding a "Morning" group for data occurring before 12 PM EDT, and an "Afternoon" group for data occurring at or after 12 PM EDT. Second, column and surface data were separated by PBL height, yielding a "High PBL" group for data occurring when the PBL height was at or above 1000 m, and a "Low PBL" group for data occurring when the PBL was below 1000 m. Estimates of PBLH based on the observed potential temperature profile were again used with the P-3B analysis, while estimates derived from the WRF/CMAQ system were used with the Pandora and CMAQ analyses. The correlation within the CMAQ model for both trace gases was compared to the correlation within the observations for each of these four data groups. Lastly, the CMAQ NO_2 columns were normalized by the concurrent PBL height estimate, and the results for the correlation were re-evaluated.

5. Results and discussion

5.1. Simple linear regression analysis for P-3B, Pandora, and OMI

5.1.1. Evaluation of the correlation between column and surface for the full data set

The degree of correlation between surface mixing ratio and column abundance found from the simple linear regression analyses for the P-3B, Pandora, and OMI data sets is summarized in Table 1. To assign a degree of correlation to an analysis, the correlations for at least four of the six surface sites must have fallen within one of the categories of correlation degree. Values of R^2 are given in Table 2 (O_3 analyses) and Table 3 (NO_2 analyses), and representative scatter plots of the correlation are displayed in Fig. 3 (O_3) and Fig. 4 (NO_2). Most P-3B O_3 (Fig. A1 in Appendix A of the Supplementary Material), P-3B NO_2 (Fig. A4), Pandora O_3 (Fig. A2), and Pandora NO_2 (Fig. A5) regressions were statistically significant at a confidence level of 95% (Tables 2 and 3). The simple linear regression analyses performed with the Pandora total column O_3 and NO_2 data were not significantly different from those for the tropospheric column data. The poor correlation between OMI column O_3 or NO_2 and surface data may be partly due to the large OMI footprint size; the pixel size at nadir is 13 $\times$ 24 km^2, and increases towards the ends of the OMI swath. The OMI O_3 retrieval also loses sensitivity to the lower troposphere (Liu et al., 2010). P-3B NO_2 column_ground demonstrated larger correlation than did column_air, reflecting the influence of the surface data in the column computation; P-3B O_3 column_ground and column_air demonstrated similar values. This indicates that O_3 is vertically and horizontally better mixed than NO_2 at each site. The Aldino column_UMD correlations were not significantly different from those for column_air, but were significantly smaller than those for column_ground for both gases; this suggests that the column_air analyses were more representative of the true correlation between lower tropospheric column and the surface (Tables 2 and 3). Extended analysis of the simple linear regressions is also presented in Appendix A.

5.1.2. Evaluation of the errors of the simple linear regression model

An overview of the average error of the regressions relative to the observations for O_3 and NO_2 is presented for the P-3B data sets. The column_air- and column_ground-measured surface values were first combined into one data set, as were the regression estimated surface values for the column_air and column_ground regression analyses, before computation of the average percentage error of the regression relative to the observations. The average error for P-3B O_3 was typically less than 10% at each site, with the exception of Padonia; this was due to the presence of a very low surface observation that was not a statistical outlier. Additionally, approximately 50–75% of regression estimations fell within a $\pm$10% error of the observed value (Table 4). These results support the conclusions presented for P-3B O_3 in the previous section. The average error for the Pandora O_3 regressions, however, was much more variable among sites, and could be much larger than seen for the P-3B results. The percentage of estimations falling within $\pm$10% error was typically less than 25% (Table 5). The Durbin–Watson test statistic was used to test for the presence of autocorrelation of the residuals, which would violate the assumption of independent regression errors. All Pandora O_3 regressions demonstrated positive autocorrelation and large average errors, indicating errors in the computation of the Pandora tropospheric column O_3. This may be due to subtraction of the OMI stratospheric column, which may not be representative of the true column at each surface site due to the large OMI footprint size.

The P-3B NO_2 regressions resulted in an average percentage error relative to the observations similar to the O_3 regressions at most sites, with the exceptions of Edgewood and Essex. Less than 30% of regression estimations fell within a $\pm$10% error of the observed value except at Beltsville; a typically larger but more variable percentage fell within $\pm$50% error of the observed value (Table 4). However, the Pandora NO_2 regressions displayed larger average errors than the Pandora O_3 regressions except at Beltsville, and larger average errors than the P-3B NO_2 regressions. Approximately 50% or more of regression estimations fell within $\pm$50% error of the observed value at most sites (Table 5). Plots of the regression residuals revealed other problems with this simple linear regression analysis for P-3B and Pandora NO_2. The Durbin–Watson test statistic again indicated positive autocorrelation of the residuals in the Pandora NO_2 regressions. Histograms of column_air

Table 1
Summary of degree of correlation found from the simple linear regression analyses between column amounts and surface mixing ratios. Low correlation: R^2 = 0–0.16; Moderate: R^2 = 0.16–0.64; High: R^2 = 0.64–1.0.

	NO_2	O_3
P-3B col_air	Low	High
P-3B col_ground	Moderate	High
Pandora	Moderate	Low
OMI	Not Significant	Not Significant
CMAQ (Loughner et al.)	High	Moderate
CMAQ (NOAA)	High	High

Table 2
Summary of the R^2 statistic and F-ratio (p-value) for the P-3B and Pandora O_3 simple linear regressions.

	P-3B col_air R^2	P-3B col_ground R^2	P-3B col_air F-ratio	P-3B col_ground F-ratio	P-3B column_UMD R^2	P-3B column_UMD F-ratio	Pandora R^2	Pandora F-ratio
Aldino	0.76	0.79	112.57 (<0.001)	131.81 (<0.001)	0.73	98.99 (<0.001)	0.06	21.72 (<0.001)
Beltsville	0.83	0.88	192.10 (<0.001)	267.95 (<0.001)	–	–	0.04	12.8 (<0.001)
Edgewood	0.61	0.65	62.94 (<0.001)	77.17 (<0.001)	–	–	0.01	3.53 (0.057)
Essex	0.58	0.63	52.25 (<0.001)	61.74 (<0.001)	–	–	0.03	9.39 (0.002)
Fair Hill	0.64	0.70	72.58 (<0.001)	95.47 (<0.001)	–	–	0.16	68.98 (<0.001)
Padonia	0.65	0.72	60.25 (<0.001)	85.58 (<0.001)	–	–	0.02	8.02 (0.004)

Table 3
Summary of the R^2 statistic and F-ratio (p-value) statistic for the P-3B and Pandora NO_2 simple linear regressions.

	P-3B col_air R^2	P-3B col_ground R^2	P-3B col_air F-ratio	P-3B col_ground F-ratio	P-3B column_UMD R^2	P-3B column_UMD F-ratio	Pandora R^2	Pandora F-ratio
Aldino	0.13	0.78	4.93 (0.03)	119.58 (<0.001)	0.16	6.48 (<0.016)	0.01	4.75 (0.030)
Beltsville	0.13	0.55	6.16 (0.02)	50.44 (<0.001)	–	–	0.20	80.94 (<0.001)
Edgewood	0.02	0.56	0.62 (0.429)	43.11 (<0.001)	–	–	0.21	61.03 (<0.001)
Essex	0.05	0.37	0.812 (0.380)	9.59 (0.009)	–	–	0.29	68.57 (<0.001)
Fair Hill	0.18	0.80	4.69 (0.040)	86.40 (<0.001)	–	–	0.09	7.43 (0.009)
Padonia	0.07	0.49	2.22 (0.148)	30.70 (<0.001)	–	–	0.27	94.69 (<0.001)

residuals and Pandora NO_2 residuals demonstrated some deviation from normality at some sites. Structure is evident in the lag-1 plots of the Pandora residuals at all sites, in which each residual is plotted against the residual immediately preceding it in time, indicating graphically the presence of autocorrelation of the residuals (Fig. 5). These problems with the simple linear regression are more severe for Pandora, but further suggest that a simple linear regression is not as appropriate for NO_2 as for O_3.

5.2. Multivariate linear least squares regression analysis for the P-3B and Pandora

All P-3B O_3 column_air and column_ground regressions were significant at a confidence level of 95%, and the R^2 values demonstrated modest improvement over those for the simple linear regressions (Table 6). The average percentage errors and standard deviations were consistently smaller than for the simple linear regressions, indicating that the range of the residuals had decreased. Likewise, the percentage of estimations falling within a ±10% error of the observed value was somewhat larger than or similar to the percentage for the simple linear regression at each site (Table 7). All Pandora O_3 regressions were significant, and demonstrated larger improvement relative to the simple linear regressions than did the P-3B regressions. The average percentage errors and standard deviations were much smaller, and the percentage of cases falling within a ±10% error of the observed value much larger (Tables 8 and 9). However, the Durbin–Watson results for Essex column_air and column_ground O_3 and all Pandora O_3 indicated positive autocorrelation of residuals. Some structure and fanning behavior, in which the range of residuals either increases or decreases as the abscissa increases, was also present in plots of the residuals against inverse PBL height for Pandora, indicating limitations of this regression for the Pandora O_3 data (Fig. 6).

The regressions for P-3B NO_2 column_ground at all sites and for NO_2 column_air at half of the sites were significant at a confidence level of 95%; the R^2 values also improved (Table 6). Like the P-3B O_3 results, the average percentage error and associated standard deviation decreased relative to the simple linear regression at most sites. Most sites also saw an increased percentage of regression estimations falling within a ±10% error and ±50% error of the observed value (Table 7). The Pandora NO_2 regressions also demonstrated marked improvement in the average percentage errors and the standard deviations at most sites. However, the percentage of regression estimations falling within a ±10% error and ±50% error of the observed value demonstrated marginal improvement (Tables 8 and 9). These results indicate that both the column and inverse PBL height contain useful information for NO_2. Fewer sites displayed histograms of residuals for column_air and Pandora NO_2 that departed from normality, and fewer sites indicated autocorrelation of the residuals for Pandora. However, plots of the residuals for column_air and column_ground NO_2 against predicted surface NO_2 at Edgewood displayed some fanning structure (Fig. 6). Though some improvement to the regression model is needed, these results indicate that the inverse PBL height adds useful information for the O_3 and NO_2 regressions, and thus mixing within the PBL has an important impact on the column–surface relationship for these gases. Because future geostationary air quality satellites will capture the diurnal cycle of their observations, these results further imply that care should be taken for the impact of PBL development on column quantities.

5.3. Normalization by PBL height for the P-3B and Pandora

The normalization of Pandora column NO_2 abundances by estimates of PBL height derived from the WRF/CMAQ model system resulted in a consistently moderate degree of correlation (Table 10; Fig. 7). Normalization by PBL height also resulted in statistically significant increases in the value of R^2 relative to the Pandora full data set correlation analyses at the 95% confidence level at most sites. The P-3B column NO_2 normalization analyses presented more mixed results. Normalization of P-3B column NO_2 by estimates of PBL height derived from the observed potential temperature profile resulted in moderate correlation, when significant, for column_ground, and column_air (Table 10; Fig. 7). However, normalization did not produce significantly different results relative to the P-3B full data set correlations. The lack of improvement for the P-3B normalization analyses may be due to the "well mixed PBL" assumption inherent in the gap-filling methods used for the column computations. Because one value is held constant within the lowermost PBL, the P-3B columns likely rely on a better mixed NO_2 profile than the Pandora columns, such that normalization by PBL depth does not add as much useful information for the P-3B as it did for Pandora NO_2.

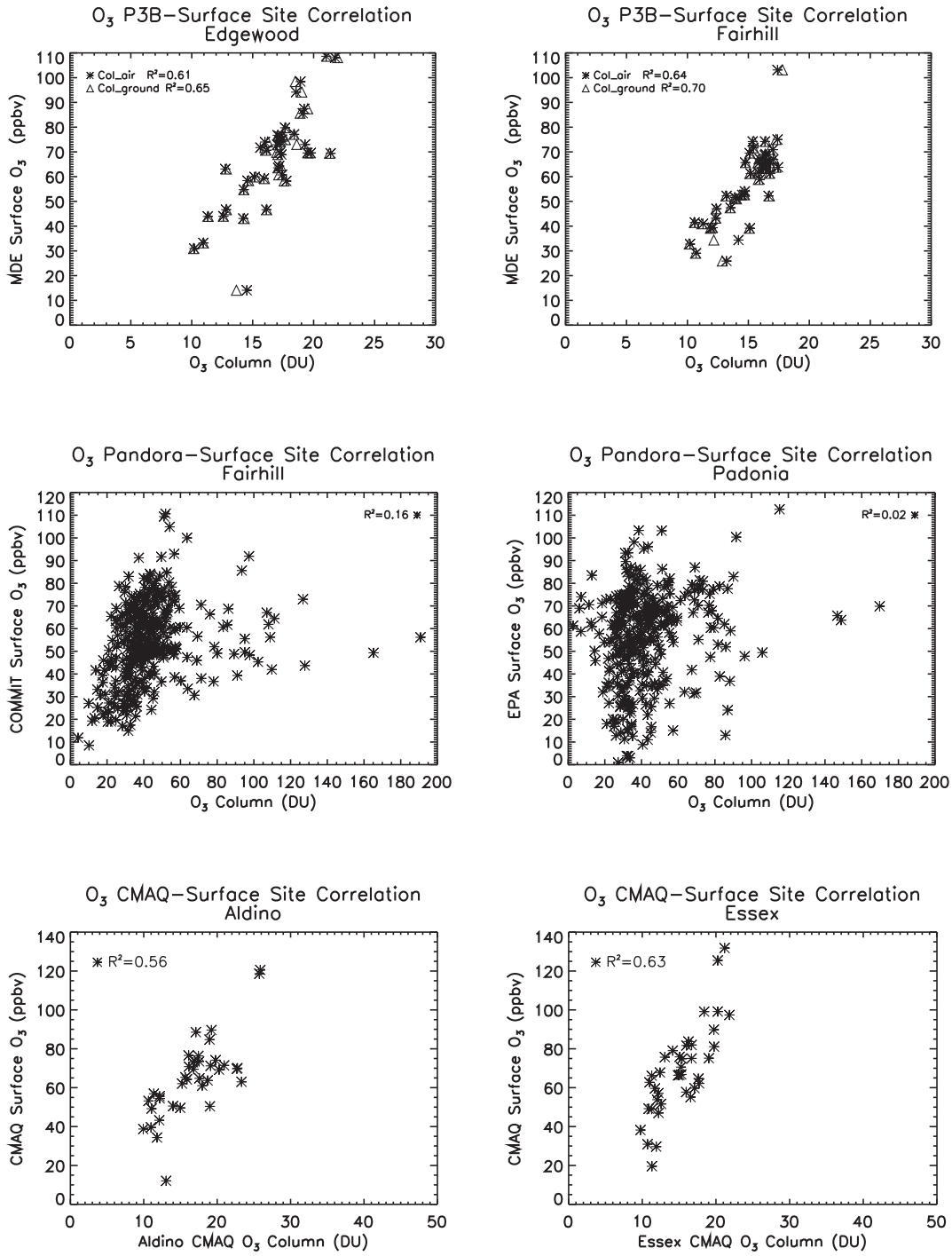

Fig. 3. Example scatter plots of O_3 column vs. surface O_3 mixing ratio for P-3B (top) Pandora (middle), and CMAQ (Loughner et al., submitted for publication, bottom) correlation analyses. Plots chosen represent the most typical behavior of the column–surface relationship for that data set. Correlation shown between all available column and surface data for each data set from the simple linear regression analysis. R^2 values displayed in the upper left corner of each plot.

The correlations between Pandora NO_2 surface mixing ratio (ppb) and column abundance (cm^{-2}) at Edgewood and Padonia presented in Section 5.1.1 compared well to the results obtained by Knepp et al. (2013) for their comparison of hourly-averaged Pandora NO_2 surface (ppb) and column data (cm^{-2}). This agreement held after Knepp et al. (2013) excluded surface NO_2 mixing ratios less than 1 ppb, and for their comparison of raw surface and column NO_2 data (see Knepp et al., 2013, Table 2). The correlations between P-3B surface mixing ratio (ppb) and column_ground (cm^{-2}) at Edgewood and Padonia also compared modestly well to Knepp et al. (2013), though the P-3B correlations were larger than either Pandora analysis. The correlations between the surface mixing ratios and Pandora or P-3B column_ground NO_2 columns normalized by PBL height presented here also compared well to the correlations obtained by Knepp et al. (2013) after application of their PBL-correction factor at Edgewood and Padonia (see Knepp et al., 2013, Table 3). Example scatter plots are presented in Fig. 7. Differences in the correlations presented here and in Knepp et al.

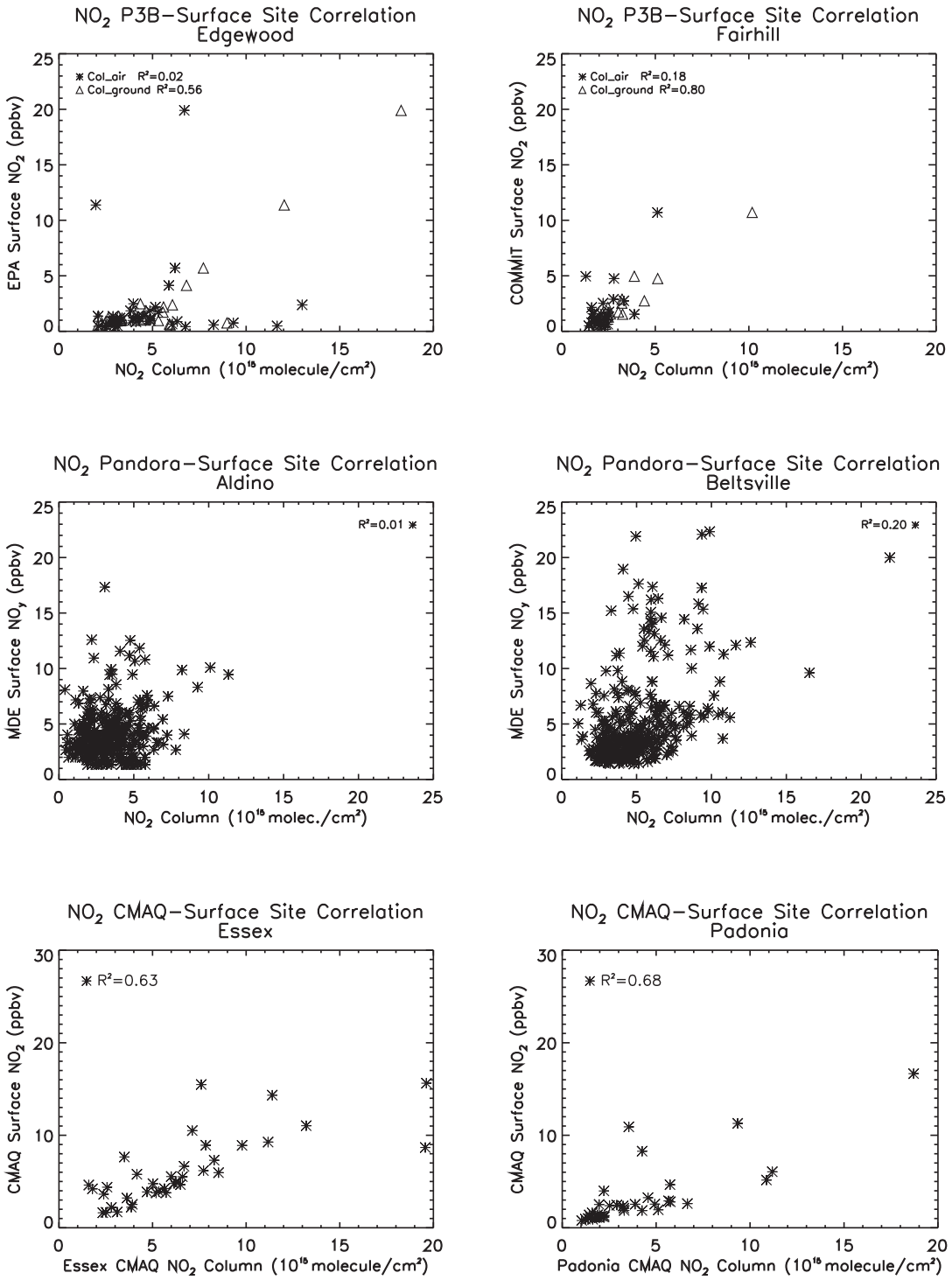

Fig. 4. Example scatter plots of NO_2 column vs. surface NO_2 mixing ratio for P-3B (top) Pandora (middle), and CMAQ (Loughner et al., submitted for publication, bottom) correlation analyses. Plots chosen represent the most typical behavior of the column–surface relationship for that data set. Correlation shown between all available column and surface data for each data set from the simple linear regression analysis. R^2 values displayed in the upper left corner of each plot.

(2013) may be due to the exclusion of data occurring at a solar zenith angle greater than 75° by Knepp et al. (2013), and differences in the PBL height derived from the WRF/CMAQ model system, the model used by Knepp et al. (2013), and from the P-3B potential temperature profile. This agreement between the results presented here and in Knepp et al. (2013) further demonstrates the influence of mixing within the PBL on the NO_2 column–surface relationship. The results presented in this section also bolster the conclusion found by Knepp et al. (2013) that, to a first order, NO_2 column abundances can be relevant to surface air quality.

5.4. Comparison of CMAQ analyses to observational analyses

The degree of correlation between surface mixing ratio and column abundance found from the simple linear regression analyses for the Loughner et al. (submitted for publication) CMAQ

Table 4
Summary of percentage errors (standard deviation) simple linear regression for all sites relative to observed surface values. Column_air and column_ground are analyzed together for each site.

	O_3 Mean error	% of cases w/in ±10% error	NO_2 Mean error	% of cases w/in ±10% error	% of cases w/in ±50% error
Aldino	3.1 (±24.6) %	61.3%	9.7 (±37.2) %	28.6%	88.5%
Beltsville	6.0 (±37.4) %	74.1%	3.2 (±18.7) %	47.7%	98.8%
Edgewood	7.1 (±44.9) %	51.2%	−58.2 (±607.3) %	0.00%	26.3%
Essex	6.1 (±38.2) %	59.7%	36.5 (±83.4) %	11.1%	52.8%
Fair Hill	2.5 (±18.8) %	63.9%	4.2 (±416.0) %	10.4%	39.6%
Padonia	40.2 (±236.8) %	61.4%	4.0 (±93.9) %	21.1%	63.6%

Table 5
Summary of percentage errors of Pandora simple linear regression for all sites relative to observed surface values.

	O_3 Mean error	% of cases w/in ±10% error	NO_2 Mean error	% of cases w/in ±10% error	% of cases w/in ±50% error
Aldino	16.9 (±66.6) %	24.8%	27.3 (±88.5) %	24.7%	81.0%
Beltsville	61.9 (±270.8) %	21.0%	20.4 (±59.6) %	22.1%	74.6%
Edgewood	29.9 (±112.9) %	23.6%	−125.5 (±2381.7%)	4.3%	28.1%
Essex	30.6 (±116.6) %	23.9%	58.1 (±374.1) %	11.2%	62.9%
Fair Hill	12.1 (±43.7) %	23.9%	−382.6 (±2554.9) %	6.8%	44.6%
Padonia	47.6 (±318.4) %	23.1%	119.5 (±941.2) %	15.4%	62.3%

model output is summarized in Table 1. Values of R^2 are given in Table 11, and representative scatter plots of the correlation are displayed in Figs. 3 and 4. All regressions were statistically significant at a confidence level of 95%. Unlike the P-3B correlations, the CMAQ O_3 correlations (Fig. A3) were not generally larger than the CMAQ NO_2 correlations (Fig. A6). Significant differences in correlation between the CMAQ and P-3B analyses occurred between CMAQ and column_air NO_2 at most sites; CMAQ generally presented larger correlation than column_air. As discussed previously, the Aldino column_UMD analysis suggested that the P-3B column_ground correlations were likely too high. The CMAQ O_3 or NO_2 correlations were also statistically significantly greater than

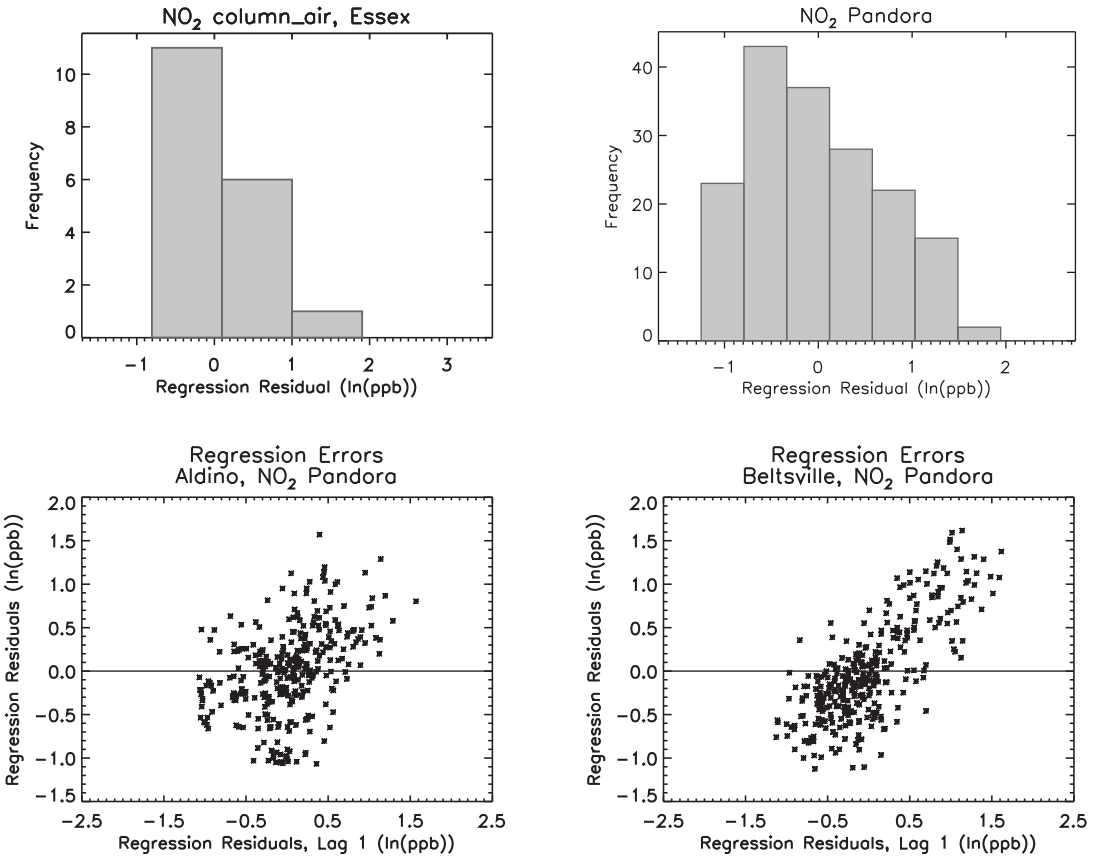

Fig. 5. Example scatter plots for NO_2 simple linear regression residuals. (top) Histograms of NO_2 residuals for Essex P-3B column_air and Pandora. (bottom) Pandora NO_2 residuals plotted against the lagged-1 residuals at Aldino and Beltsville.

Table 6
Summary of the R^2 statistic and F-ratio (p-value) for the P-3B O_3 and NO_2 multivariate regressions.

	P-3B O_3 col_air R^2	P-3B O_3 col_ground R^2	P-3B O_3 col_air F-ratio	P-3B O_3 col_ground F-ratio	P-3B NO_2 col_air R^2	P-3B NO_2 col_ground R^2	P-3B NO_2 col_air F-ratio	P-3B NO_2 col_ground F-ratio
Aldino	0.82	0.83	75.62 (<0.001)	81.87 (<0.001)	0.30	0.78	6.69 (0.003)	55.32 (<0.001)
Beltsville	0.90	0.93	169.79 (<0.001)	227.91 (<0.001)	0.44	0.66	14.88 (<0.001)	37.58 (<0.001)
Edgewood	0.67	0.70	38.36 (<0.001)	44.48 (<0.001)	0.05	0.63	0.85 (0.437)	26.47 (<0.001)
Essex	0.72	0.74	42.99 (<0.001)	47.24 (<0.001)	0.21	0.53	1.91 (0.182)	8.17 (0.009)
Fair Hill	0.66	0.69	37.64 (<0.001)	43.09 (<0.001)	0.19	0.80	2.52 (0.104)	41.53 (<0.001)
Padonia	0.74	0.78	46.66 (<0.001)	57.47 (<0.001)	0.43	0.63	11.23 (<0.001)	25.58 (<0.001)

Table 7
Summary of percentage errors of P-3B multivariate regression for all sites relative to observed surface values. Col_air and col_ground are analyzed together for each site.

	O_3 Mean error	% of cases w/in ±10% error	NO_2 Mean error	% of cases w/in ±10% error	% of cases w/in ±50% error
Aldino	2.0 (±18.2) %	54.8%	8.3 (±33.3) %	22.1%	89.7%
Beltsville	3.5 (±23.6) %	77.2%	2.2 (±15.6) %	52.4%	98.8%
Edgewood	5.8 (±34.9) %	62.2%	−89.2 (±439.3) %	5.6%	20.8%
Essex	3.9 (±24.4) %	60.3%	30.6 (±81.8) %	11.8%	61.8%
Fair Hill	2.3 (±18.6) %	67.9%	11.6 (±436.4) %	8.3%	43.8%
Padonia	26.5 (±154.1) %	58.6%	0.8 (±71.7) %	21.2%	72.8%

Table 8
Summary of the R^2 statistic and F-ratio (p-value) for the Pandora O_3 and NO_2 multivariate regressions.

	O_3 R^2	O_3 F-ratio	NO_2 R^2	NO_2 F-ratio
Aldino	0.42	130.0 (<0.001)	0.34	84.2 (<0.001)
Beltsville	0.54	201.7 (<0.001)	0.68	354.2 (<0.001)
Edgewood	0.36	89.2 (<0.001)	0.52	123.7 (<0.001)
Essex	0.25	47.7 (<0.001)	0.57	112.7 (<0.001)
Fair Hill	0.47	155.7 (<0.001)	0.27	13.5 (<0.001)
Padonia	0.51	183.3 (<0.001)	0.59	Q85.3 (<0.001)

those for Pandora O_3 or NO_2 at most sites. This indicates that O_3 and NO_2 may be too well mixed vertically and horizontally within the model.

Values of R^2 for the correlation separation analyses are given in Appendix B. Comparing the Loughner et al. (submitted for publication) CMAQ simulation to the P-3B for the correlation analyses separated by time of day, the CMAQ NO_2 correlations were significantly larger than those for P-3B NO_2 column_air for the Afternoon group at four of the six MDE sites. However, CMAQ produced significantly larger correlations relative to Pandora for the O_3 and NO_2 Afternoon analyses at all sites (Tables B1, B2, B6). The larger CMAQ NO_2 correlations relative to P-3B column_air but not column_ground for the Afternoon analysis suggests that these large CMAQ correlations during afternoon may be related to the growth of the boundary layer during the day and that too much horizontal and vertical mixing within the boundary layer is occurring in the model. For the separation by PBL height analyses, CMAQ produced correlations significantly larger than those for P-3B NO_2 column_ground for the High PBL group at three of six MDE sites, and larger than those for P-3B NO_2 column_air for both PBL data groups at all sites. CMAQ produced significantly larger correlations relative to the Pandora O_3 analyses for the Low and High PBL groups at all sites, and relative to Pandora NO_2 for both data groups at four of six sites (Tables B3, B4, B6). Because most significant differences occurred with either the Afternoon group or High PBL group, this suggests that mixing influences the column–surface relationship within CMAQ and that horizontal and vertical mixing may be too strong within the model. Furthermore, the correlation between CMAQ PBL height-normalized column NO_2 and surface NO_2 was significantly larger than the full data set correlations at only two sites; normalization by PBL height does not add as much information to the CMAQ correlations because NO_2 is too well mixed within the model (Table 12).

A high degree of correlation was found between both O_3 and NO_2 surface and column output within the NOAA CMAQ forecast (Table 1); the correlations within this forecast were significantly larger than the P-3B O_3 and NO_2 and Loughner et al. (submitted for publication) simulation correlations at several sites, and was significantly larger than all Pandora O_3 and NO_2 correlations (Table 12). The results for the correlation separation analyses for the NOAA CMAQ forecast are consistent with the results for the Loughner et al. (submitted for publication) simulation, though the impacts within the NOAA forecast were greater. For example, in addition to presenting significantly larger correlations relative to the P-3B NO_2 column_air analyses for both Low and High PBL groups, NOAA CMAQ NO_2 also produced larger correlations relative to the NO_2 column_ground analyses for the High PBL at four of six MDE sites (Tables B7 and B8). Additionally, no correlations between PBL-normalized NO_2 column and surface mixing ratios were significantly different than the full data set correlations for the

Table 9
Summary of percentage errors of Pandora multivariate regression for all sites relative to observed surface values.

	O_3 Mean error	% of cases w/in ±10% error	NO_2 Mean error	% of cases w/in ±10% error	% of cases w/in ±50% error
Aldino	0.68 (±8.6) %	82.6%	19.9 (±71.4) %	26.2%	84.6%
Beltsville	3.2 (±27.6) %	72.7%	9.8 (±39.3) %	31.0%	85.9%
Edgewood	1.4 (±13.9) %	78.9%	−131.7 (±1027.3) %	6.9%	42.4%
Essex	1.8 (±16.6) %	72.9%	38.2 (±267.3) %	17.6%	67.1%
Fair Hill	0.56 (±7.6) %	85.3%	−240.7 (±1699.0) %	5.4%	43.2%
Padonia	1.4 (±17.7) %	79.8%	62.6 (±465.0) %	17.7%	68.8%

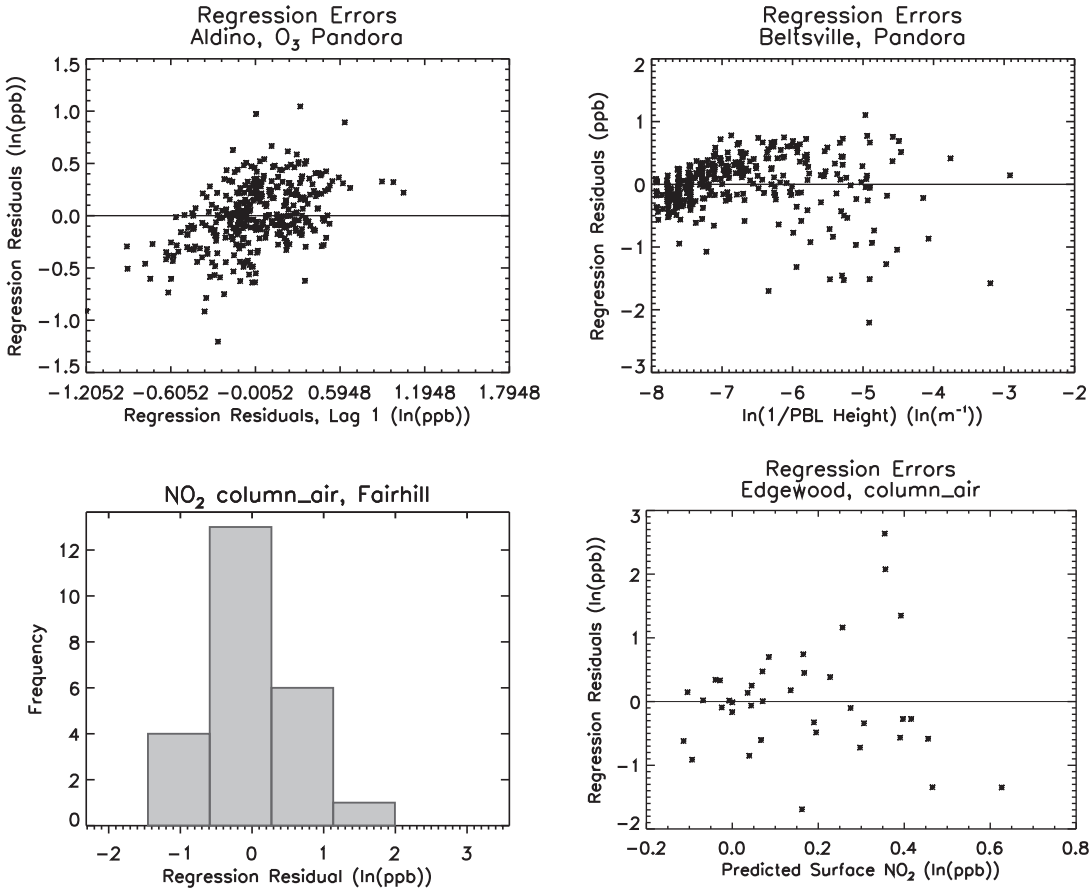

Fig. 6. Example scatter plots for O_3 and NO_2 multivariate residuals. (top) Pandora O_3 residuals plotted against lagged-1 residuals at Aldino and against the logarithm of the inverse PBL height at Beltsville. (bottom) Histogram of residuals for Fair Hill NO_2 column_air regression and plot of residuals vs. predicted surface NO_2 for Edgewood column_air regression for the multivariate regression analysis.

Table 10
Summary of the R^2 statistic for the P-3B and Pandora NO_2 PBL-normalization analysis. NS denotes non-significant correlation.

	P-3B NO_2 col_air R^2	P-3B NO_2 col_ground R^2	Pandora NO_2 R^2
Aldino	0.32	0.62	0.31
Beltsville	0.33	0.51	0.67
Edgewood	NS	0.49	0.50
Essex	NS	0.46	0.57
Fair Hill	NS	0.27	0.28
Padonia	0.37	0.61	0.58

NOAA simulation (Table 12). These results again indicate that vertical and horizontal mixing within the model may be too strong, and that inaccuracies within model mixing schemes can have an important impact on the column–surface relationship for O_3 and NO_2 within CMAQ.

6. Conclusions

A wide range of degrees of correlation resulted from the simple linear regression analyses between the O_3 and NO_2 column and

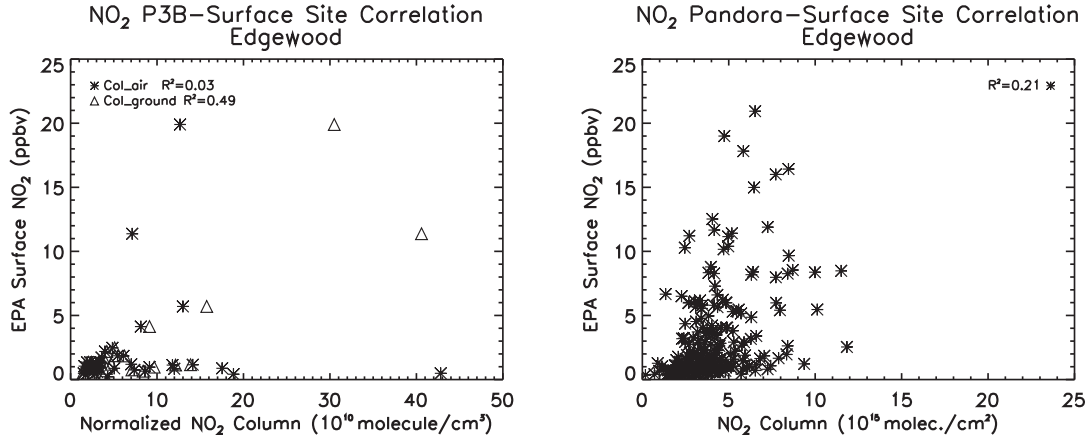

Fig. 7. Example scatter plots of NO_2 column vs. surface NO_2 mixing ratio at Edgewood for the P-3B (left) and Pandora (right). Normalization by PBL height analysis. R^2 values displayed at the top of each plot.

Table 11
Summary of the R^2 statistic and F-ratio (p-value) for the CMAQ O_3 and NO_2 simple linear regression analysis.

	CMAQ (Loughner et al.) O_3 R^2	CMAQ (Loughner et al.) NO_2 R^2	CMAQ (Loughner et al.) O_3 F-ratio	CMAQ (Loughner et al.) NO_2 F-ratio	CMAQ (NOAA) O_3 R^2	CMAQ (NOAA) NO_2 R^2	CMAQ (NOAA) O_3 F-ratio	CMAQ (NOAA) NO_2 F-ratio
Aldino	0.56	0.76	46.09 (<0.001)	46.09 (<0.001)	0.86	0.67	225.81 (<0.001)	74.01 (<0.001)
Beltsville	0.75	0.39	126.24 (<0.001)	26.58 (<0.001)	0.84	0.74	221.54 (<0.001)	117.05 (<0.001)
Edgewood	0.53	0.49	49.32 (<0.001)	42.81 (<0.001)	0.82	0.65	190.83 (<0.001)	79.50 (<0.001)
Essex	0.63	0.63	62.90 (<0.001)	63.43 (<0.001)	0.71	0.88	91.06 (<0.001)	270.38 (<0.001)
Fair Hill	0.54	0.93	48.68 (<0.001)	544.03 (<0.001)	0.83	0.88	205.91 (<0.001)	305.17 (<0.001)
Padonia	0.81	0.68	160.75 (<0.001)	78.30 (<0.001)	0.78	0.68	134.42 (<0.001)	78.13 (<0.001)

Table 12
Summary of the R^2 statistic for the CMAQ NO_2 PBL-normalization analysis. NS denotes non-significant correlation.

	CMAQ (Loughner et al.) NO_2 R^2	CMAQ (NOAA) NO_2 R^2
Aldino	0.88	0.79
Beltsville	0.85	0.67
Edgewood	0.63	0.50
Essex	0.77	0.88
Fair Hill	0.95	0.91
Padonia	0.90	0.82

surface data. The OMI tropospheric O_3 and NO_2 data resulted in non-significant correlations, the P-3B column_air NO_2 and Pandora O_3 demonstrated a low degree of correlation, P-3B column_ground NO_2, CMAQ O_3 and NO_2, and Pandora NO_2 demonstrated a moderate degree of correlation, and P-3B column_air and column_ground O_3 demonstrated a high degree of correlation with surface air quality observations. These results indicate that O_3 is generally well mixed in the vertical and horizontal, while NO_2 is not. Further, a simple linear regression model was found to fit the P-3B O_3 column and surface data well, while it struggled to capture the column versus surface relationships for the P-3B NO_2, Pandora O_3, and Pandora NO_2 data. The multivariate regression analyses and the PBL normalization correlation analyses indicate that PBL height (an indicator of mixing) add meaningful information to the column–surface relationship.

The O_3 correlations within the Loughner et al. (submitted for publication) simulation and NOAA CMAQ forecast were similar to the P-3B O_3 correlations, but were more similar to column_ground than column_air for NO_2. Both sets of CMAQ output demonstrated greater correlation between the O_3 and NO_2 column and surface during the afternoon and for conditions associated with a maturely developed PBL than did the observations. These results indicate that vertical and horizontal mixing within the model is stronger than in the observational data sets. In future work, we will investigate how the vertical mixing in CMAQ can be improved.

The large OMI footprint likely contributes to the non-significant correlations obtained between OMI tropospheric O_3 or NO_2 column and surface observations; the insufficient sensitivity of the OMI instrument to the lower troposphere also contributes for the OMI O_3 analyses. The DISCOVER-AQ measurements suggest that O_3 observations from future satellite instruments can be meaningful for surface air quality analysis if they have sufficient sensitivity to the lowest 2–3 km of the troposphere.

Acknowledgements

Funding for this work was provided by the NASA Earth Venture-1 DISCOVER-AQ project (NASA Grant NNX10AR39G). The authors thank Donald Lenschow for providing estimates of PBL height during the deployment.

Appendix A. Supplementary data

Supplementary data related to this article can be found at http://dx.doi.org/10.1016/j.atmosenv.2014.04.041.

References

Arkinson, H.L., Stehr, J.W., He, H., Brent, L.C., Loughner, C.P., Dickerson, R.R. A Transport Analysis of in Situ Airborne Trace Gas Measurements from the 2011 DISCOVER-AQ Campaign and Comparisons to CMAQ, in preparation.

Beirle, S., Platt, U., Wenig, M., Wagner, T., 2003. Weekly cycle of NO_2 by GOME measurements: a signature of anthropogenic sources. Atmospheric Chemistry and Physics 3, 2225–2232.

Boersma, K.F., Jacob, D.J., Eskes, H.J., Pinder, R.W., Wang, J., van der A, R.J., 2008. Intercomparison of SCIAMACHY and OMI tropospheric NO_2 columns: observing the diurnal evolution of chemistry and emissions from space. Journal of Geophysical Research 113, D16S26. http://dx.doi.org/10.1029/2007JD008816.

Boersma, K.F., Jacob, D.J., Trainic, M., Rudich, Y., DeSmedt, I., Dirksen, R., Eskes, H.J., 2009. Validation of urban NO_2 concentrations and their diurnal and seasonal variations observed from the SCIAMACHY and OMI sensors using in situ variations observed from the SCIAMACHY and OMI sensors using in situ surface measurements in Israeli cities. Atmospheric Chemistry and Physics 9, 3867–3879.

Bucsela, E.J., Krotkov, N.A., Celarier, E.A., Lamsal, L.N., Swartz, W.H., Bhartia, P.K., Boersma, K.F., Veefkind, J.P., Gleason, J.F., Pickering, K.E., 2013. A new algorithm for retrieval of vertical column NO_2 from nadir-viewing satellite instruments: applications to OMI. Atmospheric Measurement Techniques Discussions 6, 1361–1407.

Chance, K., Liu, X., Suleiman, R.M., Flittner, D.E., Janz, S.J., 2012. Tropospheric Emissions: Monitoring of Pollution (TEMPO), Abstract A32B-0020 Presented at 2012 Fall Meeting. AGU, San Francisco, Calif., 3–7 Dec.

Chatfield, R.B., Esswein, R.F., 2012. Estimation of surface O_3 from lower-troposphere partial-column information: Vertical correlations and covariances in ozonesonde profiles. Atmospheric Environment 61, 103–113.

Demerjian, K.L., 2000. A review of national monitoring networks in North America. Atmospheric Environment 34, 1861–1884.

Dunlea, E.J., Herndon, S.C., Nelson, D.D., Volkamer, R.M., San Martini, F., Sheehy, P.M., Zahniser, M.S., Shorter, J.H., Wormhoudt, J.C., Lamb, B.K., Allwine, E.J., Gaffney, J.S., Marley, N.A., Grutter, M., Marquez, C., Blanco, S., Cardenas, B., Retama, A., Ramos Villegas, C.R., Kolb, C.E., Molina, L.T., Molina, M.J., 2007. Evaluation of nitrogen dioxide chemiluminescence monitors in a polluted urban environment. Atmospheric Chemistry and Physics 7, 2691–2704.

Emmons, L.K., Walters, S., Hess, P.G., Lamarque, J.-F., Pfister, G.G., Fillmore, D., Granier, C., Guenther, A., Kinnison, D., Laepple, T., Orlando, J., Tie, X., Tyndall, G., Wiedinmyer, C., Baughcum, S.L., Kloster, S., 2010. Description and evaluation of the Model for Ozone and Related chemical Tracers, version 4 (MOZART-4). Geoscientific Model Development 3, 43–67.

Fishman, J., Bowman, K.W., Burrows, J.P., Richter, A., Chance, K.V., Edwards, D.P., Martin, R.V., Morris, G.A., Pierce, R.B., Ziemke, J.R., Al-Saadi, J.A., Creilson, J.K., Schaack, T.K., Thompson, A.M., 2008. Remote sensing of tropospheric pollution from space. Bulletin of the American Meteorological Society 89, 805–821.

Fishman, J., Iraci, L.T., Al-Saadi, J., Bontempi, P., Chance, K., Chavez, F., Chin, M., Coble, P., Davis, C., DiGiacomo, P., Edwards, D., Eldering, A., Goes, J., Herman, J., Hu, C., Jacob, D., Jordan, C., Kawa, S.R., Key, R., Liu, X., Lohrenz, S., Mannino, A., Natraj, V., Neil, D., Neu, J., Newchurch, M., Pickering, K., Salisbury, J., Sosik, H., Subramaniam, A., Tzortziou, M., Wang, J., Wang, M., 2012. The United States' next generation of atmospheric composition and coastal ecosystem measurements: NASA's Geostationary Coastal and Air Pollution Events (GEO-CAPE) Mission. Bulletin of the American Meteorological Society 93, 1547–1566.

Grosjean, D., Harrison, J., 1985. Response of chemiluminescence NOx analyzers and ultraviolet ozone analyzers to organic air pollutants. Environmental Science & Technology 19, 862–865.

He, H., Loughner, C., Stehr, J., Arkinson, H., Brent, L., Follette-Cook, M., Tzortziou, M., Pickering, K., Thompson, A., Martins, D., Diskin, G., Anderson, B., Crawford, J., Weinheimer, A., Lee, P., Hains, J., Dickerson, R.R., 2014. An elevated reservoir of air pollutants over the Mid-Atlantic States during the 2011 DISCOVER-AQ campaign: airborne measurements and numerical simulations. Atmospheric Environment 85, 18–30.

Herman, J., Cede, A., Spinei, E., Mount, G., Tzortziou, M., Abuhassan, N., 2009. NO_2 column amounts from ground-based Pandora and MFDOAS spectrometers using the direct-sun DOAS technique: intercomparisons and application to OMI validation. Journal of Geophysical Research Atmospheres 114. http://dx.doi.org/10.1029/2009JD011848.

Janjic, Z.I., 1994. The step-mountain eta coordinate model: further developments of the convection, viscous sublayer, and turbulence closure schemes. Monthly Weather Review 122, 927–945.

Knepp, T., Pippin, M., Crawford, J., Szykman, J., Long, R., Cowen, L., Cede, A., Abuhassan, N., Herman, J., Fishman, J., Martins, D., Stauffer, R., Thompson, A., Delgado, R., Berkoff, T., Weinheimer, A., Neil, D., 2013. Towards a methodology for estimating surface pollutant mixing ratios from high spatial and temporal resolution Retrievals, and its applicability to high-resolution space-based observations. Journal of Atmospheric Chemistry. http://dx.doi.org/10.1007/s10874-013-9257-6.

Kim, P.S., Jacob, D.J., Liu, X., Warner, J.X., Yang, K., Chance, K., Thouret, V., Nedelec, P., 2013. Global ozone–CO correlations from OMI and AIRS: constraints on tropospheric ozone sources. Atmospheric Chemistry and Physics 13, 9321–9335. http://dx.doi.org/10.5194/acp-13-9321-2013.

Lamsal, L.N., Martin, R.V., van Donkelaar, A., Steinbacher, M., Celarier, E.A., Bucsela, E., Dunlea, E.J., Pinto, J.P., 2008. Ground-level nitrogen dioxide concentrations inferred from satellite-borne Ozone Monitoring Instrument. Journal of Geophysical Research 113, D16308. http://dx.doi.org/10.1029/2007JD009235.

Lamsal, L.N., Martin, R.V., van Donkelaar, A., Celarier, E.A., Bucsela, E.J., Boersma, K.F., Dirksen, R., Luo, C., Wang, Y., 2010. Indirect validation of tropospheric nitrogen dioxide retrieved from the OMI satellite instrument: Insight into the seasonal variation of nitrogen oxides at northern midlatitudes. Journal of Geophysical Research 115, D05302. http://dx.doi.org/10.1029/2009JD013351.

Lamsal, L.N., Martin, R.V., Padmanabhan, A., van Donkelaar, A., Zhang, Q., Sioris, C.E., Chance, K., Kurosu, T.P., Newchurch, M.J., 2011. Application of satellite observations for timely updates to global anthropogenic NO_x emission inventories. Geophysical Research Letters 38, L05810. http://dx.doi.org/10.1029/2010GL046476.

Lee, C.J., Brook, J.R., Evans, G.J., Martin, R.V., Mihele, C., 2011. Novel application of satellite and in-situ measurements to map surface-level NO_2 in the Great Lakes region. Atmospheric Chemistry and Physics 11, 11761–11775.

Liu, X., Bhartia, P.K., Chance, K., Spurr, R.J.D., Kurosu, T.P., 2010. Ozone profile retrievals from the Ozone Monitoring Instrument. Atmospheric Chemistry and Physics 10, 2521–2537.

Loughner, C.P., Follette-Cook, M., Tzortzio, M., Pickering, K.E., Goldberg, D., Satam, C., Weinheimer, A., Crawford, J.H., Mannino, A., Knapp, D.J., Montzka, D.D., Diskin, G.B., Marufu, L.T., Dickerson, R.R., 2013. Impact of bay breeze circulations on surface air quality and boundary layer export. Atmospheric Environment, submitted for publication.

Martin, R.V., 2008. Satellite remote sensing of surface air quality. Atmospheric Environment 42, 7823–7843.

Natraj, V., Liu, X., Kulawik, S.S., Chance, K., Chatfield, R., Edwards, D.P., Eldering, A., Francis, G., Kurosu, T.P., Pickering, K., Spurr, R., Worden, H., 2011. Multispectral sensitivity studies for the retrieval of tropospheric and lowermost tropospheric ozone from simulated clear sky GEO-CAPE measurements. Atmospheric Environment 45, 7151–7165. http://dx.doi.org/10.1016/j.atmosenv.2011.09.014.

Ordóñez, C., Richter, A., Steinbacher, M., Zellweger, C., Nüß, H., Burrows, J.P., Prévôt, A.S.H., 2006. Comparison of 7 years of satellite-borne and ground-based tropospheric NO_2 measurements around Milan, Italy. Journal of Geophysical Research 111, D05310. http://dx.doi.org/10.1029/2005JD006305.

Pleim, J.E., 2006. A simple, efficient solution of flux-profile relationships in the atmospheric surface layer. Journal of Applied Meteorology and Climatology 45, 341–347.

Pleim, J.E., 2007. Combined local and non-local closure model for the atmospheric boundary layer. Part I: model description and testing. Journal of Applied Meteorology and Climatology 46, 1383–1395.

Steinbacher, M., Zellweger, C., Schwarzenbach, B., Bugmann, S., Buchmann, B., Ordóñez, C., Prévôt, A.S.H., Hueglin, C., 2007. Nitrogen oxide measurements at rural sites in Switzerland: bias of conventional measurement techniques. Journal of Geophysical Research Atmospheres, D11307. http://dx.doi.org/10.1029/2006JD007971.

Skamarock, W.C., Klemp, J.B., Dudhia, J., Gill, D.O., Barker, D.M., Duda, M.G., Huang, X., Wang, W., Powers, J.G., 2008. A Description of the Advanced Research WRF Version 3. NCAR Tech. Note NCAR/TN-475+STR, 113 pp..

Taubman, B.F., Marufu, L.T., Piety, C.A., Doddridge, B.G., Stehr, J.W., Dickerson, R.R., 2004. Airborne characterization of the chemical, optical, and meteorological properties, and origins of a combined ozone-haze episode over the eastern United States. Journal of the Atmospheric Sciences 61, 1781–1793.

Xiu, A., Pleim, J.E., 2001. Development of a land surface model. Part I: application in a mesoscale meteorological model. Journal of Applied Meteorology 40, 192–209.

Yarwood, G., Rao, S., Yocke, M., Whitten, G., 2005. Updates to the Carbon Bond Chemical Mechanism: CB05. Final Report to the US EPA, RT-0400675. Available at. : http://www.camx.com/publ/pdfs/CB05_Final_Report_120805.pdf.